

# Journal Pre-proof

The terpenic diamine GIB24 inhibits the growth of *Trypanosoma cruzi* epimastigotes and intracellular amastigotes, with proteomic analysis of drug-resistant epimastigotes

Camila Maria Azeredo, Mauricio Frota Saraiva, Maristela Ribeiro de Oliveira, Gisele Barbosa, Mauro Vieira de Almeida, Marcus Vinicius Nora de Souza, Maurilio José Soares

PII: S0009-2797(20)30616-5

DOI: <https://doi.org/10.1016/j.cbi.2020.109165>

Reference: CBI 109165

To appear in: *Chemico-Biological Interactions*

Received Date: 10 April 2020

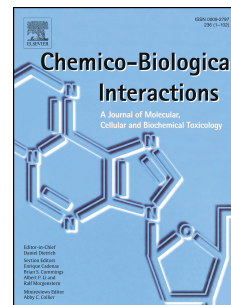
Revised Date: 18 May 2020

Accepted Date: 5 June 2020

Please cite this article as: C.M. Azeredo, M.F. Saraiva, M.R. de Oliveira, G. Barbosa, M.V. de Almeida, M.V.N. de Souza, Maurilio.José. Soares, The terpenic diamine GIB24 inhibits the growth of *Trypanosoma cruzi* epimastigotes and intracellular amastigotes, with proteomic analysis of drug-resistant epimastigotes, *Chemico-Biological Interactions* (2020), doi: <https://doi.org/10.1016/j.cbi.2020.109165>.

This is a PDF file of an article that has undergone enhancements after acceptance, such as the addition of a cover page and metadata, and formatting for readability, but it is not yet the definitive version of record. This version will undergo additional copyediting, typesetting and review before it is published in its final form, but we are providing this version to give early visibility of the article. Please note that, during the production process, errors may be discovered which could affect the content, and all legal disclaimers that apply to the journal pertain.

© 2020 Published by Elsevier B.V.



#### Author Statement

The authors contributed equally to the present work. They were divided into two groups: Mauricio Frota Saraiva, Marcus Vinicius Nora de Souza, Mauro Vieira de Almeida, Gisele Barbosa, Maristela Ribeiro de Oliveira, who worked on the synthesis and characterization of this series of compounds. And the second group: Camila Maria Azeredo and Maurílio José Soares, who tested and made the proteomic analysis of the molecule.

1 **The terpene diamine GIB24 inhibits the growth of *Trypanosoma cruzi* epimastigotes and**  
2 **intracellular amastigotes, with proteomic analysis of drug-resistant epimastigotes**

3  
4 Camila Maria Azeredo<sup>1</sup>, Mauricio Frota Saraiva<sup>2</sup>, Maristela Ribeiro de Oliveira<sup>2</sup>, Gisele  
5 Barbosa<sup>3</sup>, Mauro Vieira de Almeida<sup>3</sup>, Marcus Vinicius Nora de Souza<sup>4</sup>, Maurilio José Soares<sup>1</sup>

6  
7 1. Laboratory of Cell Biology, Carlos Chagas Institute/Fiocruz-PR, Curitiba-PR, Brazil

8 2. Institute of Physics and Chemistry, Federal University of Itajubá, Itajubá-MG, Brazil

9 3. Department of Chemistry, Federal University of Juiz de Fora, Juiz de Fora-MG, Brazil

10 4 Oswaldo Cruz Foundation, Institute of Technology in Drugs, FarManguinhos, Rio de  
11 Janeiro-RJ, Brazil

12 Corresponding Author:

13 Mauricio Frota Saraiva

14 Laboratório de Síntese de Moléculas Bioativas - LASIMBIO

15 Centro de Estudos Investigação e Inovação em Materiais Biofuncionais e Biotecnologia

16 Instituto de Física e Química-IFQ

17 Universidade Federal de Itajubá (UNIFEI)

18 Avenida BPS, 1303

19 Pinheirinho

20 37500-903 Itajubá - MG

21 Brazil

22 email: mauriciosaraiva@unifei.edu.br

23  
24 **ABSTRACT**

25 The effect of *N*-geranyl-ethane-1,2-diamine dihydrochloride (GIB24), a synthetic  
26 diamine, was assayed against different developmental forms of the parasitic protozoan  
27 *Trypanosoma cruzi* (strain Dm28c). The compound was effective against culture epimastigote  
28 forms (IC<sub>50</sub>/24h=5.64 μM; SI=16.4) and intracellular amastigotes (IC<sub>50</sub>/24h=12.89 μM;  
29 SI=7.18), as detected by the MTT methodology and by cell counting, respectively. Incubation  
30 of epimastigotes for 6h with 6 μM GIB24 (IC<sub>50</sub>/24h value) resulted in significant dissipation  
31 of the mitochondrial membrane potential, prior to permeabilization of the plasma membrane.  
32 Rounded epimastigotes with cell size reduction were observed by scanning electron  
33 microscopy. These morpho-physiological changes induced by GIB24 suggest an incidental  
34 death process. Treatment of infected Vero cells did not prevent the intracellular amastigotes  
35 from completing the intracellular cycle. However, there was a decrease in the number of

36 released parasites, increasing the ratio amastigotes/trypomastigotes. Proteomic analysis of 15  
37  $\mu\text{M}$  GIB24 resistant epimastigotes indicated that the compound acts mainly on mitochondrial  
38 components involved in the Krebs cycle and in maintaining the oxidative homeostasis of the  
39 parasites. Our data suggest that GIB24 is active against the main morphological forms of *T.*  
40 *cruzi*.

41  
42 **Key words:** Diamine, terpenoid, geraniol, *Trypanosoma cruzi*.

#### 43 44 HALLMARKS

- 45 - The diamine GIB24 (IS=7.18) showed high selective activity against intracellular  
46 amastigotes of *T. cruzi*.
- 47 - Flow cytometric analysis showed that GIB-24 induced dissipation of the mitochondrial  
48 membrane potential reduced the cell size and led to phosphatidylserine exposure in treated  
49 epimastigotes. The data suggest that GIB-24 cause incidental cell death in *T. cruzi*.
- 50 - Analysis of the proteome of 15  $\mu\text{M}$  GIB-24 resistant epimastigotes indicated that GIB-24  
51 acts preferentially on proteins involved in metabolism, mitochondrial functions, and oxidative  
52 stress control. Further experiments are needed to clarify how differentially expressed proteins  
53 communicate.
- 54 - GIB-24 appears as a promising compound for further evaluation against *T. cruzi*. Additional  
55 studies on synthetic derivatives of GIB-24 could produce a compound with reduced  
56 cytotoxicity and increased activity against *T. cruzi*.

#### 57 58 1. INTRODUCTION

59 Chagas disease is a chronic systemic parasitosis caused by the  
60 protozoan *Trypanosoma cruzi* (Euglenozoa: Kinetoplastea). It estimated that there are  
61 currently six to seven million people infected in the world, most of them in Latin America,  
62 where the disease is endemic (WHO, 2016). This disease is considered a zoonosis since the  
63 natural reservoirs are marsupials and placental mammals that occur in the American  
64 continent. In humans, the disease results from the invasion of natural ecotypes, as well as the  
65 establishment of the insect vectors in human dwellings due to the socio-economic conditions  
66 of poor rural populations, where the disease is endemic (Urbina, 2010). Due mainly to the  
67 emigration of chronically infected people from Latin America, in the last decades, Chagas  
68 disease has been found more frequently in non-endemic countries, such as the United States  
69 of America, Canada, countries of the European continent and some Western Pacific countries  
70 (Basile et al., 2011; Blumental et al., 2015; Requena-Méndez et al., 2015; Urbina, 2010;

71 WHO, 2016). Two empirically determined imidazo-heterocyclic derivatives emerged in the late  
72 1960s to be the only drugs used to treat Chagas disease: Benznidazole and Nifurtimox. Both  
73 currently used in the acute phase, and their efficacy is limited and variable during the chronic  
74 phase of the illness (Bermudez et al., 2016; Maya et al., 2007; Urbina, 2010; Urbina, 2015).  
75 Furthermore, both drugs are toxic, with several side effects. An effective, single-dose, non-  
76 toxic, and low-cost drug with use in both the treatment of patients and the prevention of  
77 Chagas disease is still a goal to be achieved. Therefore, there is a demand for the research and  
78 evaluation of new compounds that may be active on *Trypanosoma cruzi* (Romanha et al.,  
79 2010; Alviano et al., 2012). The search for biologically active substances more effective and  
80 less toxic than benznidazole, coming from different natural and synthetic sources, such as  
81 compounds based on polyamines (diamines). Natural polyamines, such as putrescine,  
82 spermidine, and spermine, are organic cations in eukaryotic and prokaryotic cells. These  
83 compounds are essential for cell growth and differentiation (Reigada et al., 2016; Yamanaka  
84 et al., 2013). Therefore, compounds based on this class could interfere with the metabolism or  
85 function of polyamines being an excellent strategy to find new drugs against this disease  
86 (Yamanaka et al., 2013). Polyamines can be obtained by de novo synthesis from ornithine  
87 and, in some cases, arginine, or transported from the extracellular medium (Colotti and Ilari,  
88 2011). In contrast to other protozoan parasites, *T. cruzi* is auxotrophic for polyamines. The  
89 reason for that is due to the inability to synthesize putrescine. This synthesis does not occur  
90 due to the lack of arginine (ADC) and ornithine (ODC) decarboxylase (Carrillo et al., 1999;  
91 Carrillo et al., 2003). Therefore, the intracellular availability of polyamines in *T.*  
92 *cruzi* depends exclusively on the transport processes (Reigada et al., 2016). Some polyamine  
93 biosynthesis inhibitors have already produced clinically useful tools, particularly for the  
94 treatment of parasitic diseases (Yamanka et al., 2013). In this context, it can be mention  
95 pentamidine used to treat leishmaniasis. This drug inhibits the transport of polyamines in *L.*  
96 *infantum* and *T. cruzi* (O'Sullivan et al., 2015). Synthetic diamines have been evaluated as  
97 possible inhibitors of trypanothione synthase (TryS) activity. This enzyme catalyzes the  
98 binding of glutathione and spermidine to form trypanothione being essential for the redox  
99 system of trypanosomatids. For example, 6-arylpyrido [2,3-d] pyrimidine-2,7-diamine  
100 derivatives were mild inhibitors of *T. cruzi* TryS (Benitez et al. 2016). Therefore, the study of  
101 diamine derivatives is a strategy that targets the action on natural polyamines. The main target  
102 would be trypanothione and/or components of its metabolic pathway (Flohe, 2012).  
103 Considering that, several groups demonstrated the trypanocidal activity of lipidic (Sales  
104 Júnior et al., 2014), aliphatic (Yamanaka et al., 2013), lipophilic long chain diamines  
105 (Legarda-Ceballos et al., 2015). Intracellular amastigotes of *T. cruzi* were highly susceptible

106 to lipodic diamines (Sales Junior et al., 2014) and aliphatic diamines (Tamanaka et al., 2015).

107 Such data indicate that diamine derivatives could be useful prototypes for the development of  
108 more effective and more specific new drugs against *T. cruzi*. Therefore, in this work, we  
109 tested the effect of a new synthetic terpenic diamine derivative (GIB24) on the different  
110 developmental forms of *T. cruzi*. Our data show that GIB24 is active against the main  
111 morphological forms of *T. cruzi*.

## 112 113 2. MATERIAL AND METHODS

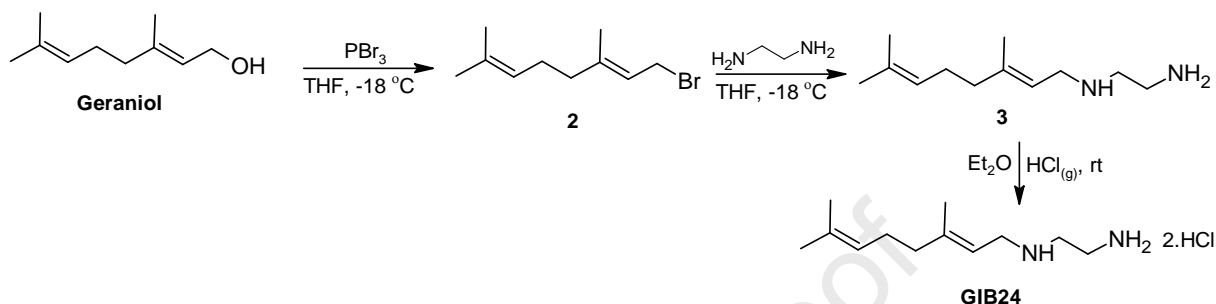
### 114 2.1 Chemistry

115 All reagents and solvents were reagent grade and were used without prior purification.  
116 All reactions were monitored by thin layer chromatography (TLC, Sigma-Aldrich® 60). The  
117 Geranyl bromide (compound **2**) were purified by liquid-liquid extraction and the  
118 geranyldiamine was purified by liquid-liquid extraction followed by flash chromatography on  
119 Sigma-Aldrich® silica gel 60 (230-400 mesh) using CH<sub>2</sub>Cl<sub>2</sub>:CH<sub>3</sub>OH:NH<sub>4</sub>OH (80:18:2) as  
120 eluent. The IR spectra were acquired on a Perkin Elmer Spectrum 100 FTIR  
121 spectrophotometer with an Attenuated Total Reflectance (ATR) attachment and only  
122 significant peaks were recorded. <sup>1</sup>H NMR (300 MHz) and <sup>13</sup>C NMR (75 MHz) spectra of the  
123 final compound (**4**) was recorded in CDCl<sub>3</sub> on a Bruker Avance ACX300 (300MHz). The  
124 chemical shifts (δ) are quoted in parts per million (ppm) downfield from the internal reference  
125 standard, tetramethylsilane (TMS), and the coupling constants (*J*) were recorded in Hertz.  
126 Splitting pattern abbreviations are as follows: s = singlet, brs = broad singlet, d = doublet, t =  
127 triplet and m = multiplet. ESI-HRMS mass spectra were carried out on a Bruker MicroTOF  
128 spectrometer.

#### 129 130 2.1.1 Synthesis of GIB24

131 Sixteen terpenic diamines were previously screened against intracellular amastigotes  
132 of *T. cruzi* (data not shown). From these, only GIB24 presented a satisfactory Selectivity  
133 Index (SI) and therefore it was selected for further analyses. The synthesis of terpenic diamine  
134 *N*-geranyl-ethane-1,2-diamine dihydrochloride (**GIB24**) was made according to the literature  
135 (dos Reis et al., 2016) (Scheme 1). The terpenic alcohol, (*E*)-3,7-dimethylocta-2,6-dien-1-ol **1**  
136 was converted into their respective bromide **2** by treatment with phosphorus tribromide (PBr<sub>3</sub>)  
137 in tetrahydrofuran (THF). The allyl bromide **2** was then reacted with an excess of the ethane-  
138 1,2-diamine in dichloromethane at -18 °C for 24 hours to provide the intermediate  
139 compound **3** in 58% yield. The transformation of terpenic diamine **3** in your respective  
140 hydrochloride salt was prepared by using a solution containing **3** in diethyl ether. In another

141 flask, sulfuric acid was added dropwise over sodium chloride with vigorous stirring. The  
 142 gaseous hydrochloric acid was bubbled in diamine **3** solution. After twenty minutes, the  
 143 formation of a precipitate was observed. The solution remained under agitation and bubbling  
 144 for more 10 minutes. Finally, the precipitate was filtered under reduced pressure to furnish a  
 145 white solid, compound **GIB24** in 95% of yield. This final compound was confirmed using <sup>1</sup>H  
 146 NMR, <sup>13</sup>C NMR, and ESI-HRMS.



147  
 148

149 **Scheme 1:** Synthesis of *N*-geranyl-ethane-1,2-diamine dihydrochloride (**GIB24**).

150

### 151 2.1.2 Characterization of **GIB24**

152

#### 153 (*E*)-*N*<sup>1</sup>-(3,7-dimethylocta-2,6-dien-1-yl)ethane-1,2-diamine dihydrochloride (**GIB24**)

154

155

156

157

158

159

160

161

162

white solid (yield: 1.6 g, 95%). **FTIR** (ATR, cm<sup>-1</sup>): 3220 (ν, N-H<sub>3</sub><sup>+</sup>), 2937 (ν<sub>as</sub>, CH<sub>2</sub>), 2886 (ν<sub>s</sub>, CH<sub>3</sub>), 2704, 2592 and 2435 (ν, NH<sup>+</sup>), 1674 (ν, C=C), 1606 (δ<sub>as</sub>, NH<sub>3</sub><sup>+</sup>), 1532 (δ<sub>s</sub>, NH<sub>3</sub><sup>+</sup>), 1454 (δ<sub>s</sub>, CH<sub>2</sub>), 1378 (δ<sub>s</sub>, CH<sub>3</sub>), 1027 (ν, C-N), 809 (γ, =C-H). **<sup>1</sup>H NMR** ((CD<sub>3</sub>)<sub>2</sub>SO, 300 MHz) δ (ppm): 1.57 (s, 3H, CH<sub>3</sub>), 1.64 (s, 3H, CH<sub>3</sub>), 1.70 (s, 3H, CH<sub>3</sub>), 2.04 (m, 4H, 2xCH<sub>2</sub>), 3.17 (brs, 4H, 2xCH<sub>2</sub>), 3.58 (d, 2H, CH<sub>2</sub>, *J* = 7,3 Hz), 5.09 (m, 1H, CH), 5.28 (t, 1H, CH, *J* = 7.0 Hz), 8.51 (brs, 3H, NH<sub>3</sub>), 9.50 (brs, 2H, NH<sub>2</sub>). **<sup>13</sup>C NMR** ((CD<sub>3</sub>)<sub>2</sub>SO, 75 MHz) δ (ppm): 16.5 (CH<sub>3</sub>), 17.6 (CH<sub>3</sub>), 25.5 (CH<sub>3</sub>), 25.8 (CH<sub>2</sub>), 35.3 (CH<sub>2</sub>), 39.1 (CH<sub>2</sub>), 43.2 (CH<sub>2</sub>), 44.2 (CH<sub>2</sub>), 114.4 (CH), 123.6 (CH), 131.2 (C), 144.1 (C). **HRMS:** *m/z* calculated for C<sub>12</sub>H<sub>24</sub>N<sub>2</sub> [M+H]<sup>+</sup> 197.2012, found 197.2004.

163

164

## 164 2.2 Biology

165

166

167

168

169

### 169 2.2.1 Reagents

170 Fetal calf serum was purchased from Cultivar (Campinas, SP, Brazil). Ribonuclease-123  
171 and propidium iodide were purchased from Invitrogen (Carlsbad, CA, USA). Trypsin was  
172 purchased from Promega (Madison, WI, USA). Giemsa stain, L-glutamine, MTT, DMEM  
173 medium, benznidazole and DMSO were purchased from Sigma-Aldrich (St. Louis, MO,  
174 USA).

#### 175 176 2.2.2 Vero Cells

177 Vero cells (ATCC: CCL-81) were used in the assays to determine cytotoxicity and  
178 trypanocidal activity against intracellular amastigote forms. Cell cultures were maintained at  
179 37°C in a humidified CO<sub>2</sub> atmosphere, in 75 cm<sup>2</sup> culture flasks containing DMEM medium  
180 (pH 7.4) supplemented with 10% fetal bovine serum (FBS), 2 mM L-glutamine, 100 µg/mL  
181 streptomycin and 100 IU/mL penicillin. The cell cultures were kept by weekly subcultures in  
182 this same medium.

183 For the bioassays, cell monolayers were washed with phosphate buffered saline (PBS,  
184 pH 7.2), trypsinized and collected by centrifugation at 100 g for 4 minutes. Cell concentration  
185 was adjusted to 10<sup>6</sup> cells/mL in DMEM medium + 10% FBS and the cells were then seeded in  
186 96 well plates (2x10<sup>4</sup> cells/well) for the cytotoxicity assays, or in 24 well plates (6x10<sup>4</sup>  
187 cells/well) for the antiparasitic activity assays. After 24h the cell cultures were used in the  
188 bioassays.

#### 189 190 2.2.3 Parasites

191 *Trypanosoma cruzi* clone Dm28c was used in all experiments. Culture epimastigotes  
192 were kept at 28°C in LIT medium containing 10% FBS, with passages at every three days.

193 Cell-derived trypomastigotes were obtained from previously infected Vero cell  
194 cultures. After 3-4 days of infection the trypomastigotes present in the culture supernatant  
195 were collected, centrifuged for 10 min at 3000 g, suspended in DMEM + 10% FBS and used  
196 either for a new infection or for the drug assays.

197 In order to obtain intracellular amastigotes, Vero cells cultures were infected with cell  
198 derived trypomastigotes (ratio 10 parasites per cell). After four hours of interaction the  
199 monolayers were washed twice with PBS for removal of non-internalized parasites. The  
200 infected cultures were kept for 12h at 37°C and 5% CO<sub>2</sub> atmosphere in culture flasks  
201 containing DMEM medium + 10% FBS, and then used in the drug assays.

202

## 203 2.2.4 Cytotoxicity Assays

204 Vero cell cultures were incubated for 24h at 37°C with different concentrations (20 to  
205 500 µM) of GIB-24. Cell viability was then determined by the MTT colorimetric assay, by  
206 incubation with 50 µL MTT (at 2 mg/ml in PBS). The plates were wrapped in foil and then  
207 for 3h incubated at 37°C. The medium was then removed by abrupt reversal of the plate and  
208 100 µL DMSO was added. After solubilization of the formazan crystals the optical density  
209 (O.D.) reading was carried out at 550 nm in EL800 ELISA reader (Biotek, Winooski, VT,  
210 USA). The CC<sub>50</sub>/24h value (cytotoxic concentration for 50% of the population) was estimated  
211 from the mean values of technical triplicates by non-linear regression using GraphPad Prism  
212 5.0 software.

213

## 214 2.2.5 Effect of GIB-24 on epimastigotes

215 Three-day-old culture epimastigotes were suspended in LIT medium at  $1 \times 10^7$  cells/mL  
216 and then incubated at 28°C in 96-well plates containing different concentrations of GIB24 (1  
217 to 500 µM). Benznidazole and 1% DMSO were used as positive and negative controls,  
218 respectively. The antiparasitic activity was evaluated by the MTT technique. After the  
219 incubation period, 50 µL MTT (at 10 mg/mL in PBS) was added to all wells, the plate was  
220 wrapped in foil was incubated at 37°C. After 3h the plate was centrifuged for 10 min at 500g  
221 and the medium was removed by abrupt reversal of the plate. The parasite pellet was  
222 resuspended in 20 µL of 10% SDS in 0.01 M HCl and this solution was incubated at 37°C for  
223 1 hr, or until lysis of all parasites. Then 80 µL of DMSO was added to all wells and the plate  
224 was again incubated at 37°C with manual shaking at every 15 min until complete  
225 solubilization of the formazan crystals. The O.D. reading was carried out at 550 nm in a  
226 Biotek EL800 ELISA reader.

227 The IC<sub>50</sub> value (inhibitory concentration for 50% of the parasite population) was  
228 estimated from the mean values obtained from triplicate experiments, with GraphPad Prism  
229 5.0 software. The Selectivity Index (SI) was calculated by dividing the cytotoxic  
230 concentration obtained in Vero cells (CC<sub>50</sub>/24h) by the inhibitory concentration in  
231 epimastigote forms (IC<sub>50</sub>/24h).

232

## 233 2.2.6 Effect of GIB24 on intracellular amastigotes

234 Infected Vero cells containing intracellular amastigotes were incubated with different  
235 concentrations (3.75 to 100 µM) of GIB24. Benznidazole and 1% DMSO were used as

236 controls. After 24 hours the cell culture plates were washed with PBS, fixed with methanol  
237 and stained for 30 minutes with Giemsa diluted in PBS pH 7.2.

238 Evaluation of trypanocidal activity was made by random counting of 100 host cells per  
239 plate well with the aid of ImageJ software, from images obtained in an inverted microscope.  
240 The number of infected cells and the number of intracellular amastigotes were evaluated in an  
241 experiment performed in technical triplicate. The values were expressed as percent inhibition  
242 (PI), as calculated using the following formula:  $PI = 100 - (T / C \times 100)$ , where T is the mean  
243 number of total intracellular amastigotes in treated cells and C is the mean number of total  
244 intracellular amastigotes in control cells. The  $IC_{50}/24h$  value was then estimated from the PI  
245 values with the CompuSyn software, by using the concentration-effect data.

#### 246 247 2.2.7 Effect of GIB24 on cell-derived trypomastigotes

248 Cell-derived trypomastigotes were washed in PBS (by centrifugation at 3000 g for 10  
249 min) and then incubated for 4h at 37°C in a 5% CO<sub>2</sub> atmosphere with GIB24 diluted at  
250 different concentrations (3 to 25 µM) in DMEM + 10% FBS. After this period the number of  
251 trypomastigotes was counted in Neubauer chamber and the percentage of parasite inhibition  
252 in treated wells relative to untreated wells (control with 1% DMSO) was calculated. The  
253 concentration-effect data were analyzed with CompuSyn software to calculate the  $IC_{50}/4h$  for  
254 trypomastigotes.

#### 255 256 2.2.8 Effect of GIB24 on the release of intracellular parasites

257 Vero cells previously seeded in 24 well plates ( $1 \times 10^5$  cells per well) were infected with  
258  $1 \times 10^6$  cell-derived trypomastigotes. After incubation for 4h the cell monolayers were washed  
259 with PBS for removal of non-internalized parasites and then 1 ml of DMEM + 10% FBS was  
260 added to each well. After incubation for 12h at 37°C and 5% CO<sub>2</sub> atmosphere the compound  
261 GIB24 was added at different concentrations (5 to 13 µM). After 72 hours the trypomastigotes  
262 and amastigotes released into the supernatant were collected and counted in Neubauer  
263 chamber. The percent inhibition of total released cells (trypomastigotes + amastigotes)  
264 relative to the control was used to calculate the  $IC_{50}/72h$  value, by using the CompuSyn  
265 software. Furthermore, the relative percentage of trypomastigotes and amastigotes released in  
266 treated and untreated cultures was also quantified, by using the Excel software.

#### 267 268 2.2.9 Effect of GIB24 on medium pH

269 A 24-well plate was prepared containing pure DMEM medium, as well as infected and  
270 uninfected Vero cell cultures in DMEM medium. Then, 5 to 13 µM GIB-24 was added to the

271 wens, in order to evaluate whether GIB24 would modify the pH of the culture medium.  
272 Measurements were performed after 48h of incubation using an ORION 520A-X pH meter.  
273 The experiment was performed in technical duplicate. Statistical analyzes were performed  
274 using GraphPad Prism 5.0 software.

275

#### 276 2.2.10 Flow Cytometry

277 Culture epimastigotes ( $1 \times 10^6$  cells) were pre-treated for 24h with 3,6 ( $IC_{50}/24h$ ) or 12  
278 ( $2 \times IC_{50}/24h$ )  $\mu M$  of GIB24, centrifuged for 1 min at 7000 g, washed with PBS and then  
279 processed for flow cytometry as described below.

280 For cell membrane permeability assays, the parasites were resuspended in PBS  
281 containing 5  $\mu g/ml$  propidium iodide (PI). After 15 min at 28°C the cells were immediately  
282 quantified without washing in a FACSCanto II cytometer. Parasites were considered dead  
283 when positively labeled, using a 585/42 nm filter. As a positive control, epimastigotes were  
284 permeabilized with 0.125% saponin, which was added to the sample after the PI labeling.  
285 About collected 20,000 events (SSC×FSC scatter, ungated) were collected and the data were  
286 analyzed using the FlowJo software (Treestar, Ashland, OR, USA).

287 To evaluate the mitochondrial membrane potential, the parasites were incubated for 15  
288 min at 28°C with 10  $\mu g/mL$  rhodamine 123, washed 3 times in PBS and quantitated in a  
289 FACSCanto II cytometer using the 530/30 nm filter. About 20,000 events (SSC×FSC scatter,  
290 ungated) were collected. As a control, epimastigotes were treated with 200  $\mu M$  carbonyl  
291 cyanide m-chlorophenyl hydrazine (CCCP) after the rhodamine labeling. The data were  
292 analyzed using the FlowJo software.

293 Apoptosis was evaluated by quantification of the phosphatidylserine exposure with the  
294 BD PharMingen Annexin V-FITC Apoptosis Detection kit, according to manufacturer's  
295 instructions. Briefly, the cells were stained for 30 min at 28°C with annexin-V-FITC and then  
296 stained for 15 min at 28°C with propidium iodide. In all analyzes, 20,000 events were  
297 collected at the gate corresponding to epimastigotes (FSC×SSC scatter). Annexin-V labeling  
298 was observed with the 530/30 nm filter and propidium iodide with the 585/42 nm filter. The  
299 data were analyzed using the FlowJo software.

300

#### 301 2.2.11 Scanning electron microscopy (SEM)

302 After incubation in LIT medium containing the  $IC_{50}/24h$  value of GIB24,  
303 epimastigotes were collected by centrifugation for 1 min at 9300 g and washed in PBS. The  
304 cells were fixed for 40 minutes with 2.5% glutaraldehyde in 0.1 M phosphate buffer pH 7.2,  
305 washed in 0.1 M cacodylate buffer pH 7.2 and adhered on coverslips coated with 0.1% poly-

306 L-lysine. It followed post-fixation for 10 min with 1% osmium tetroxide, dehydration in  
307 increasing acetone series (30, 50, 70, 90 and 100%) and critical point drying. The coverslips  
308 were adhered in SEM stubs and coated with a 20 nm-thick gold layer. The sample was  
309 observed in a Jeol JSM 6010PLUS-LA scanning electron microscope.

#### 310 311 2.2.12 Selection of GIB24 resistant epimastigotes

312 Epimastigotes were selected in LIT medium containing increasing concentrations of  
313 GIB24 (3 to 15  $\mu\text{M}$ ), with passages at every 4-5 days. The drug concentration was increased  
314 at every 15 days, until reaching 15  $\mu\text{M}$ . Such selection was performed in biological duplicate.  
315 The parasites were maintained at this concentration for 5 months and then a growth curve was  
316 daily evaluated (starting with  $1 \times 10^6$  epimastigotes/ml) for both biological replicates by  
317 countings in Neubauer chamber, until to the 8<sup>th</sup> day. Furthermore, it was made a flow  
318 cytometric evaluation of plasma membrane integrity and mitochondrial membrane potential  
319 of 3-day-old resistant cultures, as described above. Untreated epimastigotes and wild  
320 epimastigotes treated for 3 days with 15  $\mu\text{M}$  GIB24 were used as a control.

#### 321 322 2.2.13 Proteomics of GIB-24 resistant epimastigotes – Protein extract preparation

323 Two biological replicates of wild epimastigotes and two biological replicates of 15  $\mu\text{M}$   
324 GIB-24 resistant epimastigotes were cultured for 3 days. Then,  $3 \times 10^8$  cells were centrifuged  
325 for 5 min at 5000 *g* and washed twice with PBS. It followed addition of 240  $\mu\text{l}$  of lysis buffer  
326 (4% SDS, 100 mM DTT, 100 mM Tris-HCl, pH 7.5) and the samples were heated for 3 min  
327 at 95°C. The samples were left for 1 h in a sonicator bath to break the DNA and then  
328 centrifuged for 5 min at 20000 *g* at 20°C. The supernatant was collected and stored at -70°C  
329 until use.

330 The samples were thawed and processed for FASP (Filter-Aided Sample Preparation)  
331 as previously described (Wisniewski et al., 2009). Each sample was first packed in an Amicon  
332 Ultra-15 10K centrifugal filter unit (Merck Millipore, Barueri, SP, Brazil), about 5 mg protein  
333 per filter. An UA solution (8 M Urea in 100 mM Tris-HCl pH, 8.8 + 10 mM dithiothreitol)  
334 was then added to each Amicon filter. The samples were homogenized and centrifuged for  
335 three times at 4000 *g* for 30 minutes at 20°C. It followed alkylation for 1 min with 50 mM  
336 iodoacetamide in UA, incubation in the dark for 20 min and centrifugation for 40 min at 4000  
337 *g* at 20°C. Two wash steps were then performed with UA, followed by two wash steps with  
338 50 mM ammonium bicarbonate (ABC), with centrifugation for 30 min at 4000 *g*.

339 The extracts were then dosed in a Qubit 2.0 fluorometer (Life Technologies, Carlsbad,  
340 CA, USA). Trypsin (1  $\mu\text{g}$  trypsin per 100  $\mu\text{g}$  protein), and ABC solution were then added,

341 with incubation for 10h at 57 °C. After elution of the digested peptides with ABC, it followed  
342 homogenization and centrifugation for 40 min at 4000 g at 20°C. The samples were then  
343 resuspended in 0.5 M NaCl, followed by homogenization and centrifugation for 40 min at  
344 4000 g at 20°C. Finally, the peptides were dosed at 280 nm in a NanoDrop ND-1000  
345 equipment (Thermo Fisher Scientific, Waltham, MA, USA) and acidified with 0.5%  
346 trifluoroacetic acid.

#### 347 348 2.2.14 Proteomics of GIB24 resistant epimastigotes - Peptide fractionation

349 After protein digestion the peptides were fractionated by basic reverse phase liquid  
350 chromatography, using Sep Pack C18 130 mg columns. The columns were activated with 5  
351 mL methanol and equilibrated with 5 mL of 20 mM ammonium formate (FA: 0.8%  
352 ammonium hydroxide + 0.16% formic acid). About 10 mL for each peptide sample was  
353 passed through the column and the column was washed twice with 5 mL of 20 mM FA.  
354 Peptide elution was performed with different concentrations of acetonitrile (ACN) into  
355 different flasks: 1 mL of 10% ACN/20 mM FA for the first, 1 mL of 14% ACN/20 mM FA  
356 for the second, 1 mL of 18% ACN/20 mM FA for the third flask and 1 ml of 60% ACN/20  
357 mM FA for the last flask. The elutions were then dosed in a Qubit fluorometer.

358 All fractions were dried in Speed Vac (~ 10 hours) and then stored in Stage-tips  
359 manufactured by inserting a piece of C18 activated membrane into a P200 pipette tip. The  
360 C18 membrane was activated with 100 µL methanol and equilibrated with 200 µL of solution  
361 A (1% trifluoroacetic acid in water), with centrifugations for 6 min at 1000 g. The Speed-Vac  
362 dried peptides were resuspended in 1 mL of solution A and then passed through the C18  
363 membrane by centrifugation at 1000 g. About 10 µg peptide was added per Stage-tip, which  
364 were washed twice with 200 µL solution A, centrifuged for 6 min at 1000 g and then stored at  
365 4°C until elution.

#### 366 367 2.2.15 Proteomics of GIB24 resistant epimastigotes – Analysis by Nano LC-MS/MS

368 Peptides in each Stage-tip were eluted by washing with 200 µL of solution, and  
369 collected by centrifugation for 6 minutes at 1000 g. The peptides were transferred to new  
370 tubes and eluted twice with 20 µL of solution B (1% trifluoroacetic acid in 80% acetonitrile).  
371 Acetonitrile was removed by Speed-Vac drying (approximately 30 minutes, without heating).  
372 The peptides were then resuspended in 12.5 µL of solution ATD (5% acetonitrile, 1%  
373 trifluoroacetic acid, 5% DMSO) for injection in the chromatography, where they were  
374 separated and entered into the mass spectrometer for analysis.

375 The samples were analyzed in duplicate, by injection of 4 µg peptides per run. The  
376 peptide mixtures were separated by reversed phase liquid nanocromatography and analyzed  
377 by nano ESI MS/MS. The experiments were performed with an EASY-nLC 1000  
378 chromatograph (Thermo Scientific) coupled to the Orbitrap XL ETD (Thermo Scientific)  
379 LTQ mass spectrometer equipped with a Phoenix ST ionization source. Peptide separation  
380 occurred with a flow of 250 nL/min in mobile phase with acetonitrile (ACN)/0.1% formic  
381 acid/5% DMSO. A linear gradient of 5 to 40% ACN was used in 120 minutes.  
382 Chromatography was performed on a 30 cm silica analytical column with internal diameter of  
383 75 µm and C18 particles (Dr. Maisch HPLC GmbH, Ammerbuch-Entringen, Germany) with a  
384 diameter of 1.9 µm heated to 60°C. The peptides were ionized by nano electro spray (at 2.7  
385 kV) and injected into the MS. The acquisition mode was determined by Data Dependent  
386 Analysis (DDA) as follows: initial scan in Orbitrap with resolution of 15.000, followed by  
387 selection of the 10 most intense ions, which were fragmented by ICD and analyzed in the ion  
388 trap.

389 In parallel to the MS/MS a full scan was performed in Orbitrap with a resolution of  
390 60.000. In the selection of ions for MS2, a dynamic exclusion list of 90 seconds was used.  
391 The lock mass option was used to obtain better accuracy of mass (error below 0.5 ppm) of  
392 tryptic peptide precursors detected by MS.

393

#### 394 2.2.16 Analysis of proteomic data

395 The generated files (raw) were analyzed with the MaxQuant algorithm, version  
396 1.5.5.1. Searches were made against a database of *Trypanosoma cruzi* protein sequences plus  
397 common contaminants, such as keratins and trypsin, together with a database composed by  
398 the reverse of the sequences used in the search. In the search parameters, a tolerance up to 20  
399 ppm (first search) and 4.5 ppm (main search) was allowed for the MS1 spectra, with tolerance  
400 of 0.5 Da for the MS2 spectra. Analysis was specific for tryptic peptides, allowing up to two  
401 missed cleavages, and peptides with a minimum size of 7 aminoacid residues. The standard  
402 MaxQuant parameters were used, as follows: *Fixed modifications*: Carbamidomethyl (C);  
403 *Variable modifications*: Acetyl (Protein N-term); *Oxidation* (M). The database used was from  
404 *Trypanosoma cruzi* CL Brener with 19,242 entries, downloaded on 08/10/2016 from Uniprot  
405 (<https://www.uniprot.org/>). The LFQ tool was used for protein quantification and the match  
406 between runs option was used to increase identifications by comparing spectra between runs.

407 The identified proteins were analyzed using Perseus software  
408 (<https://maxquant.net/perseus>). Protein classified as only identified by site, pollutants and  
409 reverse were excluded from the data structure. The remaining data were transformed to Log2

410 scale to continue the analyses (LINDO, 2014). Afterward, the analysis was performed in two  
411 approaches:

412 1) Statistical analysis of the data was performed using the Student's t-test with  $p = 0.05$  for the  
413 evaluation of differences in protein quantity (LFQ intensity) between control samples  
414 (untreated epimastigotes) and samples resistant to  $15 \mu\text{M}$  GIB24. Among the proteins with  
415 statistical difference, only those with a quantitative difference (GIB24 - Log<sub>2</sub> scale control  $\geq$   
416  $+1$  or  $\leq -1$ ) were analyzed.

417 2) The data were divided into two groups (Control and Resistant to  $15 \mu\text{M}$  GIB24) and were  
418 filtered only those proteins found in one group and absent in the other. For the analyzes were  
419 considered only those proteins that obtained LFQ intensity close to 24, an average intensity  
420 value found in all the proteins in this identification. Samples close to this mean value were  
421 more reliable as correctly identified, because low LFQ values represent poorly abundant  
422 proteins that may not be detected at all runs. Therefore, in proteins with LFQ intensity close  
423 to the average of all proteins, the observed difference is due to the difference in expression  
424 and not to difference in detection.

425 A Gene Ontology Consortium terms/class enrichment search was performed using  
426 TriTrypDB for all selected proteins. The Gene Ontology (GO) project provides controlled  
427 vocabulary of defined terms that represent the properties of genetic products. These cover  
428 three domains: Cell Component (GOCC, the parts of a cell or its extracellular environment),  
429 Molecular Function (GOMF, the elementary activities of a gene product at the molecular  
430 level, such as binding or catalysis), and Biological Processes (GOBP, operations or sets of  
431 molecular events with a defined beginning and end, relevant to the functioning of integrated  
432 life units: cells, tissues, organs and organisms).

433 The TriTrypDB and Pfam platforms were searched with proteins with mean intensity  
434 difference  $\geq +1$  or  $\geq -1$  (in Log<sub>2</sub>), and with proteins found in only one group (control or  
435 GIB24) in order to evaluate their possible biological functions from the identification of  
436 functional domains.

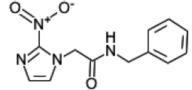
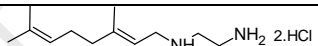
437

### 438 3. RESULTS

439 The effect of the diamine GIB24 was first evaluated on *T. cruzi* epimastigotes, by  
440 using the MTT methodology. The compound GIB24 was highly effective against these  
441 developmental forms ( $\text{CI}_{50}/24\text{h} = 5.64 \mu\text{M}$ ), but its selectivity index (SI) was lower than that of  
442 benznidazole (Table 1). Similar results were obtained for intracellular amastigotes in Vero  
443 cells, with  $\text{SI} = 7.18$  (Table 1).

444

445 Table 1. Effect of benzimidazol (BZN) and the terpenic diamine GIB24 on culture  
 446 epimastigotes (Epi) and intracellular amastigotes (Ama) of *T. cruzi*, with cytotoxicity to Vero  
 447 cells.

| Compound | IC <sub>50</sub> /24h | IC <sub>50</sub> /24h | CC <sub>50</sub> /24h | SI     | SI    | Structure   |
|----------|-----------------------|-----------------------|-----------------------|--------|-------|---|
|          | Epi<br>( $\mu$ M)     | Ama<br>( $\mu$ M)     | Vero<br>( $\mu$ M)    | Epi    | Ama   |   |
| BZN      | 12.16                 | 6.86                  | 2720                  | 223.68 | 396.5 |  |
| GIB-24   | 5.64                  | 12.89                 | 92.6                  | 16.4   | 7.18  |  |

(Oliveira et al., 2008a)

448 In order to confirm the MTT colorimetric assay, epimastigotes were treated with 3, 6  
 449 or 10  $\mu$ M GIB24 and the number of cells were evaluated 24h after treatment. It was possible  
 450 to observe a significant reduction in the number of cells as compared to the untreated control,  
 451 with about 50% less parasites in the treatment with 6  $\mu$ M GIB24 (Fig. 1).

452

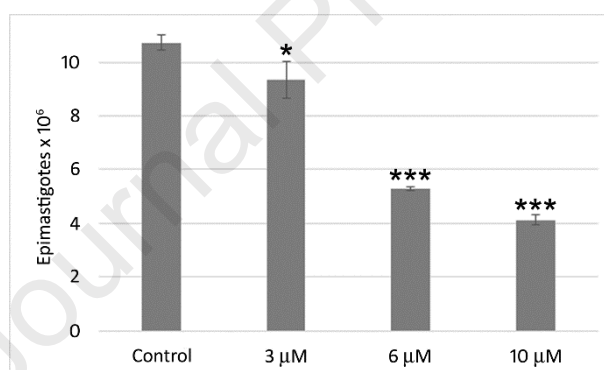


Figure 1. Total number of *T. cruzi* epimastigotes in cultures incubated for 24h with GIB24. \*\*\*  $p < 0.0001$ .

453

454 Incubation of cell-derived trypomastigotes for 4h with different GIB24 concentrations  
 455 (3 to 25  $\mu$ M) resulted in no significant lysis of the treated parasites (Fig. 2A). However, there  
 456 was a dose-dependent increase in the percentage of amastigotes found in the supernatant, with  
 457 a consequent decrease in the number of trypomastigotes (Fig. 2B). This difference was  
 458 significant ( $p < 0.05$ ) in the treatment with 25  $\mu$ M, suggesting that GIB-24 could be increasing  
 459 the rate of parasite differentiation.

460

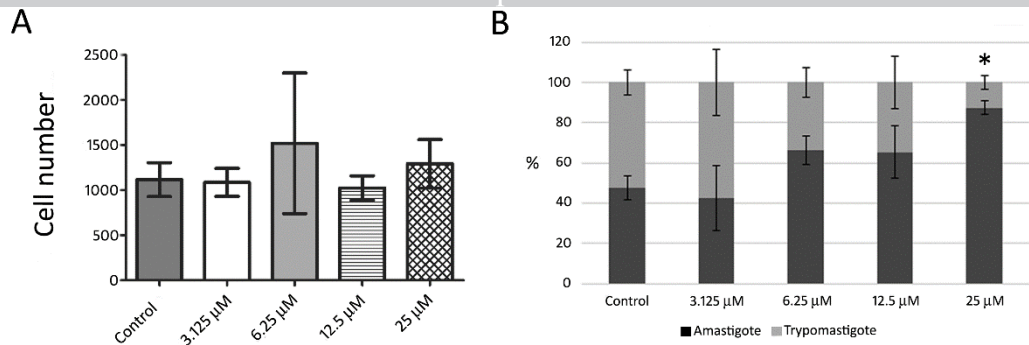


Figure 2. Number of trypomastigotes after incubation for 4h with GIB24. **A.** Mean the number of total parasites (amastigotes + trypomastigotes). **B.** Percentage of amastigotes and trypomastigotes. \* $p < 0.05$ .

461

462 The release of trypomastigotes forms was evaluated in Vero cell cultures incubated for  
 463 72h with different GIB24 concentrations (5 to 13 µM). The treatment led to a significant  
 464 decrease in the number of parasites (trypomastigotes + amastigotes) present in the supernatant  
 465 at all concentrations evaluated (Fig. 3A). Treatment with GIB24 also induced a significant  
 466 increase in the relative number of amastigotes, with a consequent decrease of trypomastigotes  
 467 in the supernatant (Fig. 3B).

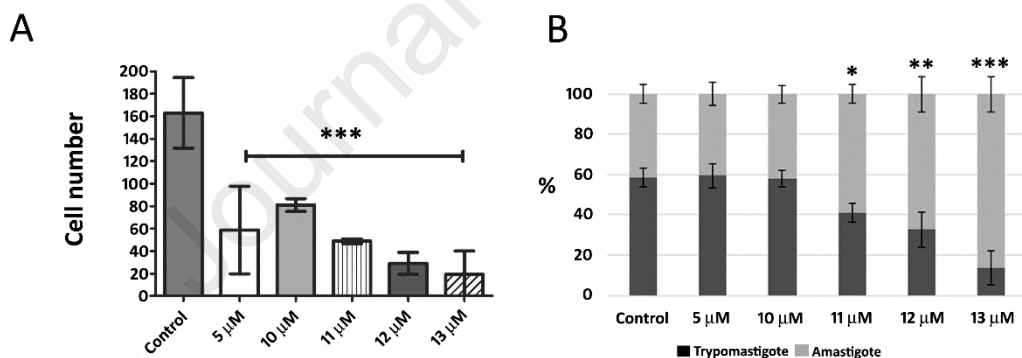
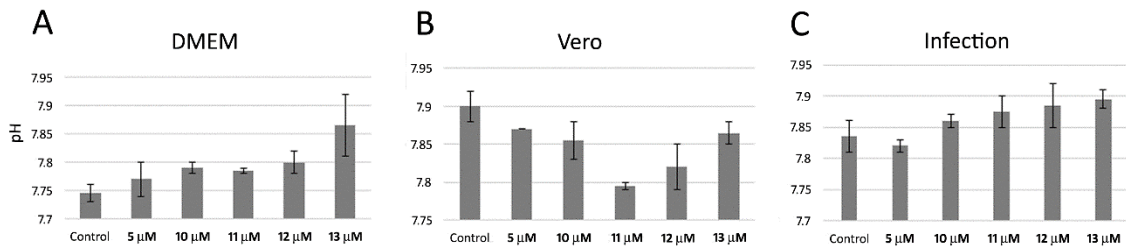


Figure 3. Effect of incubation for 72h with GIB24 on the release of parasites from Vero cells. **A.** Mean number of parasites (amastigotes + trypomastigotes) in the supernatant. **B.** Percentage of amastigotes and trypomastigotes in the supernatant. \* $p < 0.05$ ; \*\* $p < 0.01$ ; \*\*\* $p < 0.0001$ .

468

469 To exclude the possibility that GIB24 was altering the pH of treated cultures, with  
 470 consequent effect on the trypomastigote-to-amastigote differentiation, uninfected Vero cells,  
 471 infected Vero cells, and pure DMEM medium were incubated for 48 hours with 5, 10, 11, 12  
 472 or 13 µM GIB24. It was observed a tendency in alkalinization in pure DMEM and the DMEM  
 473 medium in infected Vero cell cultures, but the changes were not statistically significant (Fig.

474 4). Since GIB24 does not significantly alter the medium pH, the difference observed in the  
 475 treated cultures could be due to cellular changes promoted by the treatment.

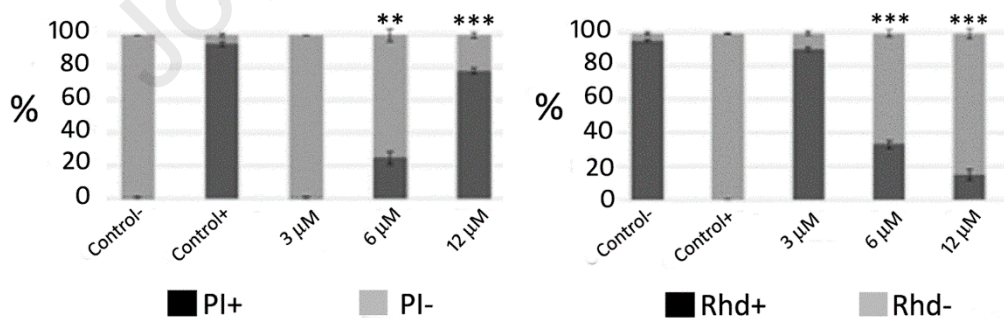


476

477 Figure 4. Effect of GIB24 on the pH of culture medium after incubation for 48h. **A.** Pure  
 478 médium; **B.** Uninfected Vero cell culture; **C.** Infected Vero cell culture.

479

480 Culture epimastigotes were incubated for 24h with 3,6 (IC<sub>50</sub>/24h) or 12 μM GIB24,  
 481 and the plasma membrane integrity was evaluated by flow cytometry using propidium iodide  
 482 (Fig. 5). Treatment for 24h with 6 μM GIB24 led to a significant increase (about 20%) in PI  
 483 labeling, as related to the negative (untreated) control (Fig. 5A). Damage to the plasma  
 484 membrane was significantly higher in parasites treated with 12 μM GIB24, when most cells  
 485 were permeable to PI and showed positive labeling. Changes in mitochondrial membrane  
 486 potential were analyzed by quantification of rhodamine-123 labeling, with non-viable cells  
 487 showing a reduction in fluorescence. GIB24-treated epimastigotes showed a significantly  
 488 reduced mitochondrial membrane potential after 24h of treatment at concentrations of 6 and  
 489 12 μM, with a significant increase in the number of negatively stained cells when compared to  
 490 the untreated control (Fig. 5B).



491

492 Figure 5. Flow cytometry analysis of *T. cruzi* epimastigotes after incubation for 24h with  
 493 GIB24. **Left Panel.** Percentage of viable epimastigotes as assessed after propide iodide  
 494 labeling. PI+= cells with damaged plasma membrane; PI-= cells with intact cell membrane.  
 495 Positive control: parasites permeabilized with 0.125% saponin. **Right Panel.** Percentage of  
 496 viable *T. cruzi* epimastigotes as assessed after rhodamine-123 labeling. Rhd-= cells with no  
 497 labeling (reduced mitochondrial membrane potential). Rhd+= cells with positive labeling  
 498 (normal mitochondrial membrane potential). Positive control: parasites treated with 200 μM

499 CCCF. Significance relative to untreated control (Control). \* $p < 0.05$ , \*\* $p < 0.01$ ,  
 500 \*\*\* $p < 0.0001$ .

501

502 Epimastigotes incubated for 24h with 6 or 12  $\mu\text{M}$  GIB24 were washed and incubated  
 503 with annexin-V-FITC and PI. Annexin-V is a protein that binds to phosphatidylserine  
 504 exposed on the surface of cells that entered the process of apoptosis (Jiménez-Ruiz et al.,  
 505 2010). Propidium iodide (PI) will only label the DNA of cells that have some membrane  
 506 discontinuity, as occurs in both late apoptosis and necrotic cells. The treatment induced a  
 507 significant increase of cells in apoptosis (Annexin+/PI-) and late apoptosis or necrosis  
 508 (Annexin+/PI+) when compared to control cultures (Table 2). When the parasites were treated  
 509 with 12  $\mu\text{M}$  GIB24 ( $2 \times \text{IC}_{50}/24\text{h}$ ) there was a significant increase in the percentage of  
 510 epimastigotes in early apoptosis (20.54 times) and in the percentage of epimastigotes in late  
 511 apoptosis/necrosis (87.72 times) when compared to control cultures (Table 2).

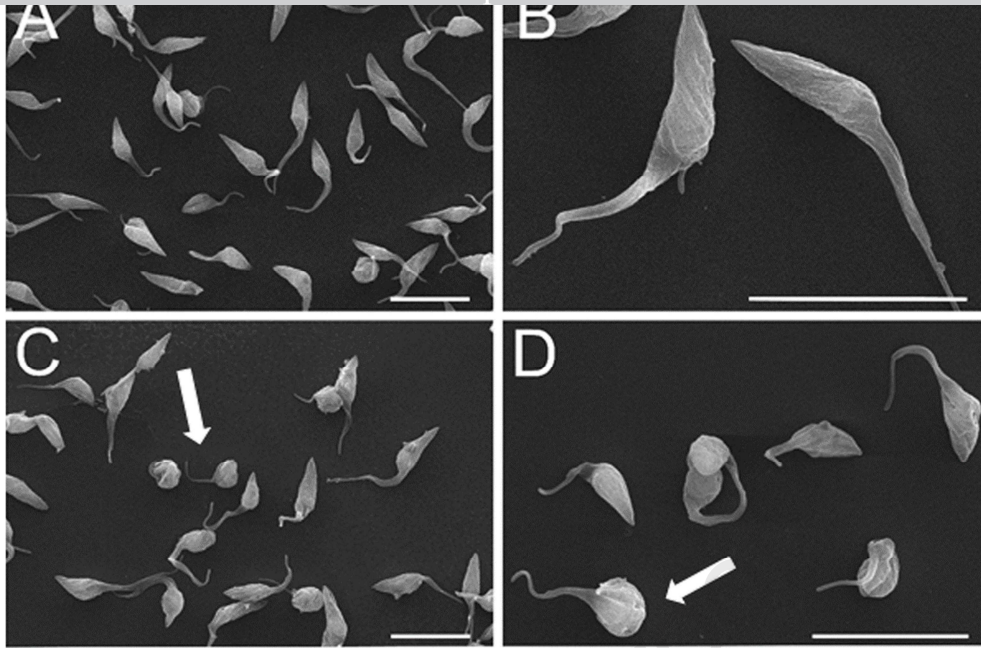
512

513 Table 2. Percentage of labeled epimastigotes after incubation for 24h with GIB-24, followed  
 514 by incubation with annexin-V-FITC and PI. Early Apoptosis: Annexin+/PI- labeled cells. Late  
 515 apoptosis/necrosis: Annexin+/PI+ labeled cells. Viable cells: Annexin-/PI-.

| <b>GIB-24</b>         | <b>Early Apoptosis</b> | <b>Late apoptosis \ Necrosis</b> | <b>Viable cells</b> |
|-----------------------|------------------------|----------------------------------|---------------------|
| Untreated control     | 0.23%                  | 0.67%                            | 99.13%              |
| 6 $\mu\text{M}$       | 0.59%                  | 2.80%                            | 96.62%              |
| Ratio Treated/control | 2.6                    | 4.18                             | 0.97                |
| 12 $\mu\text{M}$      | 4.62%                  | 57.96%                           | 37.42%              |
| Ratio Treated/control | 20.54                  | 87.72                            | 0.377               |

516

517 Analysis by scanning electron microscopy shows that untreated *T. cruzi* epimastigotes  
 518 present an elongated, fusiform body (Fig. 6A). It is possible to observe the spiral torsion of  
 519 the parasite body due to the cytoskeleton of subpellicular microtubules (Fig. 6B). Incubation  
 520 for 24h with 6  $\mu\text{M}$  GIB24 induced drastic morphological change in the parasite body, with  
 521 many parasites showing a rounded and wrinkled appearance (Fig. 6C, D).

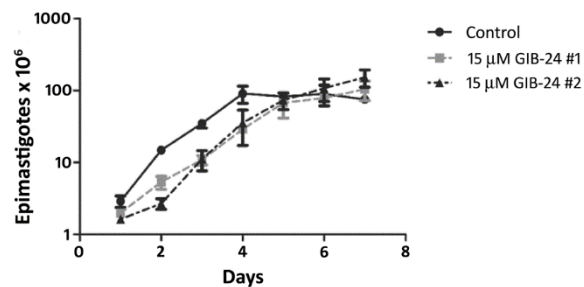


522

523 Figure 6. Scanning electron microscopy of epimastigotes treated for 24h with 6  $\mu$ M GIB24.  
 524 **A, B.** Untreated, control cells. **C, D.** Epimastigotes treated with 6  $\mu$ M GIB24. Note the  
 525 rounding of the cell body.

526

527 Resistant epimastigotes were selected by growing in cultures with increasing  
 528 concentrations of GIB24 until reaching 15  $\mu$ M (approximately  $2.5 \times IC_{50}$ / 24h). The selection  
 529 time was 2 months, followed by a further 5 months of culture in LIT medium containing 15  
 530  $\mu$ M GIB24. A growth curve showed that the resistant cultures had a growth rate similar to that  
 531 of an untreated culture (Fig. 7).



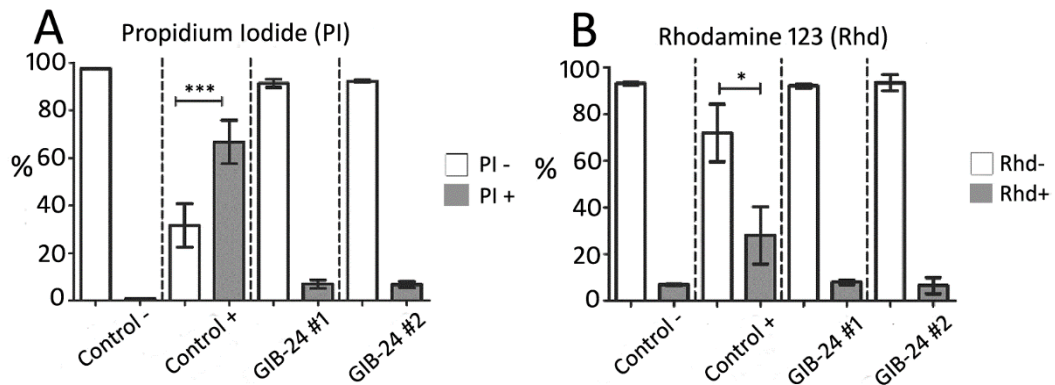
532

533 Figure 7. Growth curve of 15  $\mu$ M GIB24 resistant epimastigotes in LIT medium at 28°C, as  
 534 compared to a control, untreated culture.

535

536 Plasma membrane integrity (PI) and mitochondrial membrane potential (Rhd-123) of  
 537 epimastigotes resistant to 15  $\mu$ M GIB24 were evaluated by flow cytometry. Our data show  
 538 that membrane integrity was not significantly altered in the resistant parasites (Fig. 8A). Still,  
 539 there was a substantial decrease in viability of control, wild type epimastigotes incubated with

540 15  $\mu$ M GIB24. A similar result was observed when evaluating the mitochondrial membrane  
541 potential (Fig. 8B).



542

543 Figure 8. Evaluation of plasma membrane integrity (A) and mitochondrial membrane  
544 potential (B) in *T. cruzi* epimastigotes. Negative control: untreated cells. Positive control:  
545 wild type parasites incubated for 3 days with 15  $\mu$ M GIB24. GIB24#1 and #2: duplicate  
546 cultures of resistant epimastigotes. **A.** Percentage of parasites with undamaged (PI-) or  
547 damaged (PI+) plasma membrane. **B.** Percentage of parasites with no alteration (Rhd+) or  
548 alteration (Rhd-) in the mitochondrial membrane potential.

549

550 The proteomic analysis resulted in the identification of a total of 3954 proteins in both  
551 wild type and GIB24 resistant parasites. This number was reduced to 3810 proteins after the  
552 exclusion of contaminants and possible false identifications (Reverse/Only Identified by site).  
553 Of these, 71 proteins (Supplementary Table 3) were considered with a significant difference  
554 in expression (Student's t-test). In addition, there were five proteins found only in resistant  
555 epimastigotes (Supplementary Table 4) and five present only in the control epimastigotes  
556 (Supplementary Table 5).

557

558 GO (Gene Ontology) gene enrichment analysis of these selected 81 proteins was  
559 performed on the TritypDB, which identified a significant enrichment (p-value and  
560 Benjamini  $\leq 0.05$ ) in proteins involved with general metabolic biosynthetic processes, in  
561 mitochondrial transport and cellular homeostasis, including cellular redox homeostasis  
562 (Supplementary Table 6, GOBP Terms). The analysis also pointed to the enrichment of  
563 proteins that act as components of the plasma membrane, organelles, and mitochondrion  
564 (Supplementary Table 7, GOCC Terms). According to the enrichment of GOMF terms  
565 (molecular functions), the molecular functions are mainly involved in the transport of  
566 molecules (Supplementary Table 8, GOMF Terms).

566

567 Among the 71 proteins with a significant difference in quantity, 24 proteins were  
568 selected with a fold change  $\geq 2$  or  $\leq -2$  (or  $\geq 1$  and  $\leq -1$  when on Log<sub>2</sub> scale). Of these 24

566 proteins (Supplementary Table 5) only one is an adequately characterized protein, the KAP6.  
569 Thirteen are hypothetical proteins, and 10 are putative proteins. After searching the  
570 TriTrypDB and pFAM databases for protein identification and assignment of functional  
571 domains, the vast majority of these proteins can be grouped into the following three major  
572 groups:

573 A) Mitochondrion and Krebs cycle: KAP6 (Tc00.1047053509791.120), putative aspartate  
574 Aminotransferase (Tc00.1047053503679.10), Putative glutamate dehydrogenase  
575 (Tc00.1047053508111.30) and a cytochrome c oxidase copper chaperone (COX17;  
576 Tc00.1047053508153.994);

577 B) Generation or control of oxidative stress: hypothetical with thioredoxin domain  
578 (Tc00.1047053511181.20), hypothetical with heme-peroxidase domain  
579 (Tc00.1047053507011.130), hypothetical with thiosulfate sulfurtransferase domain  
580 (Tc00.1047053506753.130), putative alcohol dehydrogenase (Tc00.1047053511277.60);

581 C) Amino acid metabolism: Putative cytosolic leucyl aminopeptidase  
582 (Tc00.1047053509859.40), putative glutamate dehydrogenase (Tc00.1047053508111.30),  
583 hypothetical with class IV aminotransferase domain (Tc00.1047053506559.410), putative  
584 aspartate aminotransferase (Tc00.1047053503679.10).

585 When analyzing the five proteins present only in control epimastigotes and the five  
586 proteins present only in GIB24 resistant epimastigotes, it could be noted that a putative fatty  
587 acid elongase (Tc00.1047053511245.150) is present only in the resistant epimastigotes  
588 (Supplementary Table 4). while the peroxin PEX-12 (Tc00.1047053503641.19), involved  
589 with the import of proteins into the matrix of glycosomes, it is present only in the control  
590 epimastigotes (Supplementary Table 5).

591

#### 592 4. DISCUSSION

593 The terpene diamine GIB24 was effective to inhibit the growth of *Trypanosoma cruzi*  
594 culture epimastigotes and intracellular amastigotes, with  $IC_{50}/24h$  values of 5.64  $\mu M$   
595 (SI=16.4) and 12.89  $\mu M$  (SI=7.18), respectively.

596 Incubation of infected Vero cells with GIB24 led to a reduction in a number of  
597 intracellular amastigotes. As a result, there was a significant decrease in the number of  
598 released parasites (trypomastigotes + amastigotes) into the extracellular medium.  
599 Interestingly, our data showed that incubation of cell-derived trypomastigotes with GIB24  
600 resulted in no significant lysis of the parasites. However, our data showed a dose-dependent  
601 increase in the percentage of amastigotes in the supernatant, indicating that GIB24 somehow  
602 affected the amastigogenesis process (differentiation of trypomastigotes into amastigotes).

603 This event results from a relationship between environmental changes and adjustment of gene  
604 expression, which triggers this process, and can be mimicked in vitro by parasite exposure to  
605 low pH (Burchmore and Barrett, 2001; Hernandez-Osório et al., 2010; Pucci, 2009; Queiroz  
606 et al., 2014). However, no significant change in pH was observed in the culture medium used  
607 to maintain infected Vero cells treated with GIB24, excluding the hypothesis of  
608 amastigogenesis induced by pH change. This information indicated that the significant  
609 increase in number of amastigotes occurred due to a direct action of the compound on the  
610 released trypomastigotes.

611 When *T. cruzi* epimastigotes were treated with GIB24 and then analyzed by flow  
612 cytometry and scanning electron microscopy, it was possible to observe the dissipation of  
613 mitochondrial membrane potential, cell rounding (with a reduction in cell size), positive  
614 annexin V and propidium iodide labeling. These data indicated cell death by an apoptosis-like  
615 process. However, there are indications that phosphatidylserine is absent, or below the level  
616 of detection, in trypanosomatids, raising doubts about the specificity of annexin V in these  
617 parasitic protozoa. Thus, increased binding of annexin V may not necessarily be indicative of  
618 programmed cell death/apoptosis in Trypanosomatids (Proto et al., 2013).

619 Although several groups have shown the existence in trypanosomatids of phenotypes  
620 characteristic of programmed cell death/apoptosis-like/autophagy (Anjos et al., 2016;  
621 Jiménez-Ruiz et al., 2010; Sandes et al., 2004; Smirlis and Soteriadou, 2011), the existence of  
622 regulated cell death still under debated. Mainly because the biochemical pathways that  
623 precede its appearance have not yet been elucidated (Jiménez-Ruiz et al., 2010; Proto et al.,  
624 2013; Smirlis and Soteriadou, 2011). For these reasons, it has been suggested that cellular  
625 deaths identified in parasitic protozoa, such as trypanosomatids, should be classified as  
626 unregulated deaths, with two types: necrosis and incidental death (Proto et al., 2013).  
627 Incidental cell death is one that includes the cell death events that have some morphological  
628 and biochemical characteristics typical of defined (regulated) cell death processes. Therefore,  
629 the cell death identified in *T. cruzi* treated with GIB24 should be classified as incidental cell  
630 death.

631 In summary, the proteomic analysis suggests that treatment with GIB24 causes  
632 changes in mitochondrial function, generates oxidative stress, and influences the metabolism  
633 of amino acids, and lipids. Further studies are needed to demonstrate that the other identified  
634 proteins are involved in these pathways or response to stress caused by these changes. Our  
635 proteomic analysis of the differential protein expression in *T. cruzi* epimastigotes resistant to  
636 15  $\mu$ M GIB24 begins to elucidate the pathways by which the compound acts. This proteomic  
637 analysis is indicating that mitochondrial functions, amino acid metabolism, and control of

638 oxidative stress are targets of this compound. However, we can not yet claim that the  
639 compound acts specifically on the pathways involving trypanothione, as advocated for  
640 diamines in general. Further studies on the proteins differentially expressed due to the action  
641 of the compound open a perspective that should improve the understanding of how GIB24  
642 acts and how the pathways affected by the compound may be communicating. More broadly,  
643 they can support the understanding of the mechanism of action of diamines on *T. cruzi*.

644

## 645 5. ACKNOWLEDGEMENTS

646 This work was supported by Conselho Nacional de Desenvolvimento Científico  
647 (CNPq), Fundação Oswaldo Cruz (FIOCRUZ) and FAPEMIG (Project: APQ-04302-10). The  
648 authors thank the Program for technological Development in Tools for Health-PDTIS-  
649 FIOCRUZ for providing technical infrastructure (Mass Spectrometry Facility-RPT02H) and  
650 professional assistance. This work is also a collaboration research project of members of the  
651 Rede Mineira de Química (RQ-MG) supported by FAPEMIG (Project: CEX-RED-0010-14).

- 653 Alviano, D.S.; Barreto, A.L.S.; Dias, F.A.; Rodrigues, I.A.; Rosa, M.S.S.; Alviano, C.S.;  
654 Soares, R.M.A. Conventional therapy and promising plant-derived compounds against  
655 trypanosomatid parasites. **Frontiers in Microbiology**, v. 3, p. 283, 2012.
- 656
- 657 Anjos, D.O.; Alves, E.S.S.; Gonçalves, V.T.; Fontes, S.S.; Nogueira, M. L.; Suarez-Fontes,  
658 A.M.; Costa, J.B.N.; Rios-Santos, F.; Vannier-Santos, M.A. Effects of a novel belapachone  
659 derivative on *Trypanosoma cruzi*: Parasite death involving apoptosis, autophagy and necrosis.  
660 **International Journal for Parasitology: Drugs and Drug Resistance**, v. 6, p. 207-219,  
661 2016.
- 662
- 663 Basile, L.; Jansà, J.M.; Carlier, Y.; Salamanca, D.D.; Angheben, A.; Bartoloni, A.; Seixas, J.;  
664 Van Gool, T.; Cañavate, C.; Flores-Chávez, M.; Jackson, Y.; Chiodini, P.L.; Albajar-Viñas,  
665 P. Working Group on Chagas Disease. Chagas disease in European countries: the challenge of  
666 a surveillance system. **EuroSurveillance**, v. 16, n. 37, p. 19968, 2011.
- 667
- 668 Benítez, D.; Medeiros, A.; Fiestas, L.; Panozzo-Zenere, E.A.; Maiwald, F.; Prousis, K.C.;  
669 Roussaki, M.; Calogeropoulou, T.; Detsi, A.; Jaeger, T.; Šarlauskas, J.; Mašič, L. P.; Kunick,  
670 C.; Labadie, G.R.; Flohé, L.; Comini, M.A. Identification of Novel Chemical Scaffolds  
671 Inhibiting Trypanothione Synthetase from Pathogenic Trypanosomatids. **PLoS Neglected**  
672 **Tropical Disease**, v. 10, e0004617, 2016.
- 673
- 674 Bermudez, J.; Davies, C.; Simonazzi, A.; Real, J.P.; Palma, S. Current drug therapy and  
675 pharmaceutical challenges for Chagas disease. **Acta Tropica**, v. 156, p. 1-16, 2016.
- 676
- 677 Blumental, S.; Lambermont, M.; Heijmans, C.; Rodenbach, M.P.; El Kenz, H.; Sondag,  
678 D.; Bottieau, E.; Truyens, C. First Documented Transmission of *Trypanosoma cruzi* Infection  
679 through Blood Transfusion in a Child with Sickle-Cell Disease in Belgium. **PLoS Neglected**  
680 **Tropical Disease**, v. 9, e0003986, 2015.
- 681
- 682 Burchmore, R.J.; Barrett, M.P. Life in vacuoles--nutrient acquisition by *Leishmania*  
683 *amastigotes*. **International J. Parasitology**, v. 31, p. 1311-20, 2001.
- 684

- 685 Carrillo, C., Cejas, S., Gonzalez, N.S., Algranati, I.D. *Trypanosoma cruzi* epimastigotes lack  
686 ornithine decarboxylase but can express a foreign gene encoding this enzyme. **FEBS Letters**,  
687 v. 454, p.192-196, 1999.
- 688
- 689 Carrillo, C.; Cejas, S.; Huber, A.; Gonzalez, N.S.; Algranati, I.D. Lack of arginine  
690 decarboxylase in *Trypanosoma cruzi* epimastigotes. **Journal of Eukaryotic Microbiology**, v.  
691 50, p. 312-316, 2003.
- 692
- 693 Colotti G, Ilari A. Polyamine metabolism in Leishmania: from arginine to trypanothione.  
694 **Amino Acids**, v. 40, p. 269-285, 2011.
- 695
- 696 Dos Reis, D.; Souza, T. C. A.; Lourenço, M. C. S.; de Almeida, M. V.; Barbosa, A.; Eger, I.;  
697 Saraiva, M. F. Synthesis and biological evaluation against *Mycobacterium tuberculosis* and  
698 *Leishmania* of a series of diaminated terpenoids. **Biomedicine & Pharmacotherapy**, v. 84, p.  
699 1739-1747, 2016.
- 700
- 701 Flohé, L. The trypanothione system and its implications in the therapy of trypanosomatid  
702 diseases. **International Journal of Medical Microbiology**, v. 302, p. 216-220, 2012.
- 703
- 704 Hernandez-Osório, L.A.; Marquez-Due, C.; Florencio-Martinez, L. E.; Ballesteros-Rodea, G.;  
705 Martinez-Calvillo, S.; Manning-Cela, R. G. Improved Method for *In Vitro* Secondary  
706 Amastigogenesis of *Trypanosoma cruzi*: Morphometrical and Molecular Analysis of  
707 Intermediate Developmental Forms. **Journal of Biomedicine and Biotechnology**, v. p. 1-10,  
708 2010.
- 709
- 710 Jiménez-Ruiz, A.; Alzate, J.F.; Macleod, E.T.; Lüder, C.G.K.; Fasel, N.; Hurd, H. Apoptotic  
711 markers in protozoan parasites. **Parasites & Vectors**, v. 3, 104, 2010
- 712
- 713 Legarda-Ceballos, A.L.; Del Olmo, E.; López-Abán, J.; Escarcena, R.; Bustos, L.A.;  
714 Fonseca-Berzal, C.; Gómez-Barrio, A.; Dib, J.C.; Feliciano, A. S.; Muro, A. Trypanocidal  
715 Activity of Long Chain Diamines and Aminoalcohols. **Molecules**, v. 20, p. 11554-11568,  
716 2015.
- 717
- 718 LNBio, Laboratory of Mass Spectrometry, CNPEM. **Tutorial for proteome data analysis**  
719 **using the Perseus software platform** Tutorial version 1.0, January 2014.

- 720 Maya, J. D.; Cassels, B. K.; Irujo-Vasquez, F.; Ferreira, J.; Pauluez, M.; Galanti, N.;  
721 Ferreira, A.; Morello, A. Mode of action of natural and synthetic drugs against *Trypanosoma*  
722 *cruzi* and their interaction with the mammalian host. **Comparative Biochemistry and**  
723 **Physiology, Part A**, v. 146, p. 601-620, 2007.
- 724
- 725 O'Sullivan, M. C.; Durham, T. B.; Valdes, H. E.; Dauer, K. L.; Karney, N. J.; Forrestel, A.  
726 C.; Bacchi, C. J.; Baker, J. F. Dibenzosuberyl substituted polyamines and analogs of  
727 clomipramine as effective inhibitors of trypanothione reductase; molecular docking, and  
728 assessment of trypanocidal activities. **Bioorganic & Medicinal Chemistry**, v. 23, p. 996-  
729 1010, 2015.
- 730
- 731 Proto, W. R.; Coombs, G. H.; Mottram, J. C. Cell death in parasitic protozoa: regulated or  
732 incidental? **Nature Reviews Microbiology**, v. 11, p. 58-66, 2013.
- 733
- 734 Pucci, M.M. Análise proteômica da forma amastigota de populações de *Trypanosoma cruzi*  
735 sensíveis e resistentes ao benzonidazol. Dissertação (mestrado) – Dissertação para obtenção  
736 do título de Mestre em Ciências pelo Programa de Pós - Graduação em Ciências da Saúde do  
737 Centro de Pesquisas René Rachou. Área de concentração: Biologia Celular e Molecular. 119p.  
738 2009.
- 739
- 740 Queiroz, R. M. L.; Charneau, S.; Mandacaru, S. C.; Schwammle, V.; Lima, B. D.; Roepstorff,  
741 P.; Ricart, C. A. O. Quantitative Proteomic and Phosphoproteomic Analysis of *Trypanosoma*  
742 *cruzi* Amastigogenesis. **Molecular & Cellular Proteomics**, v. 13, p. 3457-3472, 2014.
- 743
- 744 Reigada, C.; Saye, M.; Vera, E. V.; Balcazar, D.; Fraccaroli, L.; Carrillo, C.; Miranda, M.R.;  
745 Pereira, C. A. *Trypanosoma cruzi* Polyamine Transporter: Its Role on Parasite Growth and  
746 Survival Under Stress Conditions. **The Journal of Membrane Biology**, v. 249, p.475-481,  
747 2016.
- 748
- 749 Requena-Méndez, A.; Aldasoro, E.; De Lazzari, E.; Sicuri, E.; Brown, M.; Moore, D. A.;  
750 Gascon, J.; Muñoz, J. Prevalence of Chagas Disease in Latin-American Migrants Living in  
751 Europe: A Systematic Review and Meta-analysis. **PLoS Neglected Tropical Disease**, v. 9, n.  
752 2, p. e0003540, 2015.
- 753

- 754 Romanha A.J., Casato S.L., Soeiro, M.N.C., Lannes-Vieira, J., Ribeiro, I., Tarvati, A.,  
755 Bourdin, B.; Blum, B.; Olivieri, B.; Zani, C.; Spadafora, C.; Chiari, E.; Chatelain, E.; Chaves,  
756 G.; Calzada, J.E.; Bustamante, J.M.; Freitas-Junior, L.H.; Romero, L.I.; Bahia, M.T.;  
757 Lotrowska, M.; Soares, M.; Andrade, S.G.; Armstrong, T.; Degraeve, W.; Andrade, Z.A. *In*  
758 *vitro* and *in vivo* experimental models for drug screening and development for Chagas  
759 disease. **Mem Inst Oswaldo Cruz**, v. 105, n. 2, p. 233-238, 2010
- 760
- 761 Sandes, J. M.; Fontes, A.; Regis-Da-Silva, C. G.; Castro M. C. A. B.; Lima-Junior, C. G.;  
762 Silva, F. P. L.; Vasconcellos, M. L. A. A.; Figueiredo, R. C. B. Q. *Trypanosoma cruzi* Cell  
763 Death Induced by the Morita-Baylis-Hillman Adduct 3-Hydroxy-2-Methylene-3-(4-  
764 Nitrophenylpropanenitrile). **PLoS ONE** v. 9, n. 4, p. e93936, 2014.
- 765
- 766 Sales Júnior, P.A.; Rezende Júnior, C. O.; Le Hyaric, M.; Almeida, M. V.; Romanha, A. J.  
767 The *in vitro* activity of fatty diamines and amino alcohols against mixed amastigote and  
768 trypomastigote *Trypanosoma cruzi* forms. **Memórias do Instituto Oswaldo Cruz**, v. 109, n.  
769 3, p. 362-364, 2014.
- 770
- 771 Smirlis, D.; Soteriadou, K. Trypanosomatid apoptosis: 'Apoptosis' without the canonical  
772 regulators. **Virulence**, v. 2, n. 3, p. 253-256, 2011.
- 773
- 774 Urbina J.A. Recent Clinical Trials for the Etiological Treatment of Chronic Chagas Disease:  
775 Advances, Challenges and Perspectives. **Journal of Eukaryotic Microbiology**, v. 62, n. 1, p.  
776 149-156, 2015.
- 777
- 778 Urbina, J.A. Specific chemotherapy of Chagas Disease: Relevance, current limitations and  
779 new approaches. **Acta Tropica**, v. 115, p. 55-68, 2010.
- 780
- 781 WHO (World Health Organization). Chagas disease (American trypanosomiasis) Fact Sheet,  
782 March 2016. Available in:  
783 < <http://www.who.int/mediacentre/factsheets/fs340/en/> > Access in: 30/03/2016
- 784
- 785 Wisniewski, J.; Zougman, A.; Mann, M. Combination of FASP and StageTip-based  
786 fractionation allows in-depth analysis of the hippocampal membrane proteome. **Journal of**  
787 **proteome research**, v. 8, n. 12, p. 5674-5678, 2009.
- 788

789 Tamaiaka, C. N.; Giordani, R. B.; Rezende Jr, C. O.; Egei, I.; Kessiel, R. L.; Tonini, M. L.,  
790 Moraes, M. H.; Araújo, D. P.; Zuanazzi, J. A.; Almeida, M. V.; Steindel, M. Assessment of  
791 Leishmanicidal and Trypanocidal Activities of Aliphatic Diamine Derivatives. **Chemical**  
792 **Biology and Drug Design**, v. 82, n. 6, p. 697-704, 2013.

Journal Pre-proof

**Highlights**

- A diamine showed high selective against intracellular amastigotes of *T. cruzi*
- Geraniol derivative reduces the cell size of *T. cruzi*. epimastigotes forms
- Geraniol derivative can cause incidental cell death in *T. cruzi*
- Terpenoid affects the mitochondrial membrane potential in epimastigote *T. cruzi*
- A Geraniol derivative as potential lead compound against *T. cruzi*

Journal Pre-proof

**Declaration of interests**

The authors declare that they have no known competing financial interests or personal relationships that could have appeared to influence the work reported in this paper.

The authors declare the following financial interests/personal relationships which may be considered as potential competing interests:

Journal Pre-proof